Modeling and Characterization of Reed Canary Grass Pellet Formation Phenomenon

Amarnath Dhamodaran, Muhammad Afzal[*]

Department of Mechanical Engineering, University of New Brunswick, Fredericton, NB, Canada E3B5A3

Email address:

d.amarnath@unb.ca (A.Dhamodaran), mafzal@unb.ca (M. Afzal)

Abstract: The behaviour of pelletized reed canary grass (RCG) with selected feedstock and process parameters was studied for variation in springback characteristics based on axial changes after the compaction process. Experiments were carried out using a uniaxial single piston cylinder assembly with a proportional integral derivative temperature controller which was built in house for research purposes. A Multiple linear regression analysis based on moisture, temperature, pressure, hold time and their interaction terms was carried out to predict the length of pellets under compression in the die and excellent correlation were obtained. A finite difference method with over relaxation technique was successfully adopted to analyse the pressure and density distributions of biomass under compressive load. The compact geometry and friction between particles and die wall had effects on the pressure and density distributions in the compacted biomass. RCG pellets with lowest expansion were subjected to axial and diametrical compression tests. Bonding and failure analysis were carried out using scanning electron microscope which showed uneven breakage and interparticle voids.

Keywords: Reed Canary Grass Pellets, Densification, Finite Difference Method, Pressure Distribution, Density Distribution, MLR Modeling

1. Introduction

An ideal energy crop is one which has low energy input, low production cost, low nutrient requirements with high yield and low amount of contaminants [1]. Cold climate limits the number of viable, high-yielding species with energy crop characteristics [2]. The quality of the biomass of grasses for use as solid fuel should have low content of water, ash, N, K, Cl and S, the ash melting temperature should be high and the biomass should have a high energy density [3]. Reed canary grass (RCG) which belongs to the subfamily *Pooideae* of the *Gramineae* family is native to the temperate regions of Europe, Asia and North America. It is normally found in wet areas like lake shores and along rivers. RCG is used as a forage crop mainly in North America, though the presence of various types and concentrations of poisonous alkaloids has restricted the use of RCG as a forage crop [4]. RCG being a persistent species grows well on most kind of soils [5]. Even though it naturally grows in wet places, it is known to be more drought resistant than many other grass species with the highest yields being obtained from organic soils. RCG with an estimated plantation life time of 10 years [6] has a compa-

ratively higher yield and single harvest system adds to its advantage.

Problems with melted ash or cinder and corrosion have often been noted while using stalky biomass for combustion which can be eliminated by the delayed harvesting [7]. During winter there is a decrease in content of elements such as K, Ca, Mg, P and Cl. This change in chemical composition is caused by leaching and leaf losses during the winter, which significantly modify the chemical and physical properties of the ash with the most relevant being an increase in the initial ash deformation temperature [8]. The delayed harvest concept, when the crop is left on field during the winter and harvested as senescent material the following spring, has helped to overcome issues like poor fuel quality. The need of expensive artificial drying excludes the summer and autumn harvest alternatives for RCG in regions with colder climatic conditions. RCG (Phalaris arundinacea L.) which is native in Canada is being considered as one of the most promising crop in bio energy industry today because of its high yield, good fuel quality and sustainability. Lower pellet production rates and variability in pellet quality has been reported in RCG pellets production due to inbuilt variabilities.

Biomass densification is a widely accepted way of converting loosely arranged forest and agricultural residues into a compressed form such as pellets, briquettes and cubes which facilitates its efficient handling, storage, transportation and usage efficiency. Setbacks like high moisture content, irregular shape and sizes, and low bulk density are eradicated by the densification process which increases the bulk density of biomass. Densification of biomass can be explained as rearranging of particles under low pressure to form close packing and removal of air located in the interstices of the bulk material during the initial stages. Closer bonds are formed during the final stages of compression based on forces of attraction between solid particles, interfacial forces and capillary pressure, adhesion and cohesion forces, solid bridges and mechanical interlocking [9, 10]. Feedstock properties and process variables are considered to have major impact on the quality of densified biomass. The timing of measurement in addition to cooling and drying conditions was identified to impact durability and strength which can be distinguished as the "green" strength (immediately after production) and the cured strength (a week later) of pellets [11]. Kaliyan and Morey [12] pointed out the role of temperature on the mean expansion in volume of densified biomass where corn stover and switchgrass from 3mm screen size with a moisture content of 8.7% expanded 12.2% and 15.6% respectively at 25°C, while their expansion was a mere 0.3% and 1.2% at 75°C. Their durability values of 96.8% and 62.9% were also the highest, which shows the effect of temperature on the mean expansion in volume. Pelleting of biomass is usually carried out by open die compaction in which the finished product is extruded from the die. The extrusion process is a continuous process, where the feedstock after densification is constantly forced through the die opening. There are three types of open die compaction presses for pellets are flat die pelleting press, ring die pelleting press and Single pelleter unit of which the first two are used in industrial scale production while the single pelleter unit is used for lab scale production.

Springback behaviour is caused by release of elastic energy stored in the material during the compaction process. In this study expansion in the axial and/or radial dimensions of a compacted granular powder material when the applied pressure is removed is attributed towards springback behaviour. Thermoplastics can react to an applied pressure either elastically, below the glass transition temperature, or viscoelastically, near or above the glass transition temperature, during the compaction process. Some degree of residual stress appears in the form of springback during the decompacting stage or the ejection of an object from a die. Spring back due to elastic recovery in fibrous materials after the densification process considerably increases the overall dimensions of the densified biomass due to expansion which happens during decompacting and ejection stage [10]. Even though a high amount of densification is obtained during compression of biomass, expansion occurs after the compressive load is released and the pellets are extruded from the die which reduces the overall bulk density. In order to acquire a better understanding towards the densification process, a study based on the role of compression characteristics and springback effect in pellet formation phenomena is of considerable importance.

Constitutive models establish relations between external stimuli on the material and its response considering the parameters of the model. They not only help in predicting the mechanical behaviour of material quantitatively but also help in giving useful inputs to computer simulations of mechanical processes, which in our case is compaction of agricultural biomass. Two main approaches of compaction modeling are micro-mechanical or discrete element method (DEM) and macro-mechanical method (Continuum method). Discrete Element Method (DEM) is a numerical modeling method that makes use of contact mechanics between the particles and between particles and the wall to model the dynamics of assemblies of particles [13, 14]. These particulate models describe how the basic physical laws affect the movement of individual powder particles. Micro-mechanical modeling describes the particle-particle and particle-wall interactions that take place when powder is compacted by considering the average number of contacts, volume fraction of particles, contact area and center-to-center distances of adjacent particles which is complex in nature. On the other hand, the macro-mechanical model treats the powder volume as a continuum. The continuum models describe how the pressure and density distributions within the compacting powder bed depend on the relevant powder properties and geometry during compaction.

A macro mechanical model includes endochronic models and rheological models [15]. Endochronic models are based more on time-dependent constitutive equations developed based on thermodynamic theory rather than plasticity. Rheological models consider ideal materials to deform in elastic, plastic and/or viscous stages where the mechanical analogues of the same are spring, friction and dashpot elements [16]. Rheological models are developed such that the model behaves qualitatively, to some degree of approximation, in a manner similar to that of the actual material. The rheological behaviours expressed are a function of stress, strain, and time which can be used to predict the mechanical behaviour of the material under various loading conditions [12]. There are a number of rheological models that could be found in the literature such as the Drucker–Prager–Cap model [17], the Cam–Clay model [18], and the DiMaggio–Sandler model [19]. These were originally developed for application in soil mechanics and geotechniques. These models have been adapted to model the compaction of metal powders [20], ceramic powders [21], and pharmaceutical powders [22–25], in biomass industry for corn stover and switchgrass by Kaliyan and Morey [12] and numerous other models involving other powder compaction industry.

Investigations show that several relationships between

compaction pressure and density have been proposed. The high number of relationships presented in the literature reflects complexity of the process. The compaction process is difficult to generalize because it depends on a large number of parameters which are hard to be completely adjustable [26]. Some models account for powder characteristics, which include particle size, shape, and surface finish, while others incorporate material properties such as hardness or plasticity [27]. Understanding the physical mechanisms that govern the powder compaction is important for compaction process. Because of this, compaction modeling has received significant attentions over the last years [28]. Macro-mechanical approach is one of the widely used modeling techniques being applied for powder compaction. The macro-mechanical model provides useful engineering information such as stress and density distribution and post-compaction shape. Mathematically, ma-cro-mechanical model is carried out by solving boundary value problem with partial differential equations for equi-librium [28, 29]. In order to analyse the variabilities affecting the pellatization process, detailed simulation is required to quantitatively analyse the pellet formation phenomena. Moreover, simulation of the pellatization process can also help to understand the influence of process parameters and provide guidance for optimization of the same.

Fracture surface analysis using scanning electron microscopy (SEM) by Stelte et al. [30] on beech pellets fracture surfaces, pressed at higher temperatures, has shown areas of cohesive failure indicating high energy failure mechanisms that are supposed to be due to lignin flow and inter-diffusion between adjacent wood particles. These were absent in both spruce and straw pellets. Infrared spectroscopy of the fracture surfaces of the straw pellets have indicated high concentrations of hydrophobic extractives, that were most likely responsible for their low compression strength, due to presence of a weak chemical boundary layer, limiting the adhesion mechanism to Vander Waals forces. Infrared spectra of the fracture surface of wood pellets, pressed at elevated temperatures, showed no signs of hydrophobic extractives. Kaliyan and Morey [31] on the SEM of corn stover and switchgrass pellets showed that the bonding between particles was created mainly through solid bridges. Ultra violet auto-fluorescence images of densified biomass have confirmed that the solid bridges were due to natural binders such as lignin and protein. They found that activating the natural binders using moisture and temperature in the range of glass transition is important to make durable particle–particle bonding. Though studies based on the kind of bridges formed in compacted biomass has been initiated, the role of temperature and moisture content in the formation of bonds needs to be studied to enhance the durability of the pellets. It would be interesting to further this study with a range of temperature, load and moisture content, to study the bonding and failure conditions.

2. Objectives

The objectives of this study are as follows:

1) To study the compression and springback behaviour of compressed RCG biomass.

2) To simulate compaction of RCG using finite difference method.

3) To evaluate the axial and diametrical strengths of pellets produced from selected feedstocks.

4) To analyze fractured pellets using scanning electron microscopy.

3. Materials and Method

RCG bales were first bone dried with the help of a conventional oven by setting the temperature at 105° C and leaving the samples in an oven for 48 hours. The bone dried material was then ground with the help of using a 1 hp model 4 Thomas-wiley mill (Thomas Scientific., Swedesboro, NJ, USA). Thus grinded material was run through a sieve test to differentiate different particle sizes in the range of 0.3 to 0.15mm and particles less than 0.15mm. According to Larsson [32] a moisture content of about 13% is found to be optimum for RCG pellets. Known moisture of 11 and 13% were added to the material and kept in an air tight container for 48 hours for even distribution of moisture before the pelleting process. Densification experiments were carried out using a uniaxial single piston – cylinder assembly which was built in house for research purposes [10].

3.1. Experiment Procedure and Conditions

In order to gain knowledge about the role of hold time on expansion in pellets three runs of 0, 15, and 30 seconds of hold time were conducted. The purpose is to point out the application of springback behaviour in a practical design problem where hold-time affects the quality of the compressed material. Two different loads of 139.3MPa (± 3MPa) and 159.2MPa (± 3MPa) were applied for producing pellets at a die speed of 0.43 mm s^{-1}. Two temperatures of 70°C (± 1°C) and 80°C (± 1°C) were selected to study the role of temperature. Three replications for the following combinations (2 pressures x 2 particle size x 2 moisture content x 2 temperature x 3 hold time) were carried out. The mean of all three replications are tabulated and analyzed. The weight of material loaded in to the die and the weight of the compacted biomass was noted along with dimensions of pellet before (length of pellet in die under compression) and after extrusion (length of extruded pellet). The length of pellet in die under compression was calculated by measuring the length of piston outside the die at the end of compression using digital calipers. Length of pellets were measured after a week's time after the pellets were allowed to cure in air tight bags at room temperature and the means were tabulated. The compression and springback characteristics of experimental pellets were studied based on three different stages. While the conditions under compression loading

were noted first, data for pellets extruded from the die immediately and after one week were also noted. The mass of material used in making RCG pellets for each run was 1.31 grams with bulk densities ranging between 208 and 250 Kg m^{-3}(Appendix A) based on particle size and moisture content. The diameter of the die used for making pellets was 8mm.

3.2. Multiple Linear Regression Modeling

In order to predict the densification of biomass based on feedstock and process variables multiple linear regression (MLR) modeling was carried out. Data sets were separated based on particle size of 0.15 to 0.30mm and particles less than 0.15mm. Pressure, moisture content, temperature and hold time were considered as independent variables to define the length of pellets under compression which was considered as a dependent variable. Analysis of variance for experimental data was carried out with interaction terms of up to three factors to find the significance of feedstock and process variables on densification of biomass. Multiple linear regression (MLR) analysis of the significant variables and interaction terms was carried out to correlate the parameters and the length of the pellet under compressive load.

The relation between the independent variables along with interaction terms and a dependent variable using the observed data with multiple linear regressions was set as follows:

$$L_{fp} = \beta_h H + \beta_p P + \beta_m M + \beta_t T + \beta_l I$$

where the dependent variable L_{fp} is the length of the pellet under compression (mm) for a given particle size; H is hold time (seconds); P is pressure (MPa); M is moisture (% wet basis); T is temperature (^{o}C), and I is the interaction term up to three factors. β_h, $\beta_p P$, $\beta_m M$, $\beta_t T$, and $\beta_l I$ are partial regression coefficients.

3.3. Biomass Compaction Modeling by Finite Difference Method

The steady state pressure distribution is governed by Laplace's equation:

$$h^2\alpha\frac{\partial^2 P}{\partial x^2} + \frac{h^2\alpha}{x}\frac{\partial P}{\partial x} - \frac{\partial^2 P}{\partial y^2} = 0 \qquad (1)$$

Were h is the aspect ratio (ratio of diameter to length of biomass under compression) and α is the radial to axial pressure ratio and P is the pressure applied [29, 26].

Steady state problems describe steady state of the system which does not vary with time. The die wall is modelled as a rigid surface and the piston was made to move at a slow rate. Thermal effects were not considered in solving this model which in turn neglects both dynamic and thermal effects. The impact of bond formation and curing of bonds between particles during compression of biomass particles is ignored in the present model.

The considered steady state model is two dimensional

representing radial (x) and axial (y) direction. Equation (1) represented as P = (x,y) was solved using the following initial and boundary conditions:

Initial condition

$$P(x, y, 0) = 0 \quad \text{at time} = 0 \qquad (2)$$

Boundary condition when time > 0 is given by

$$P(0,0) = P_a$$

Where P_a is applied pressure.
At the top of the compact

$$P(x, 0) = P_a \qquad (3)$$

Axial compacting pressure for any given depth at the central axis is given by,

$$P(0, y) = P_a * exp(-4 * \alpha * \mu * y(j)/D) \qquad (4)$$

Where μ is the friction coefficient acting between the powder and die wall and D is the diameter of the compacted biomass.

During uniaxial compaction, the upper part of the compact slides inside the die which in turn undergoes a normal load from the piston and a shear stress due to friction at the die wall [26, 33, 34].

$$P(R, y) = P_{(1,j)} * exp(-4 * \alpha * \mu * y(j)/D) + \alpha * \mu * P_a \qquad (5)$$

The amount of Pressure dissipated from top of the compact to the bottom depends on aspect ratio and coefficient of friction, which is a value defined in terms of variable which is in between 20 - 90% [26, 35-37].

$$P(x, L) = \%P_a * exp(-4 * \alpha * \mu/D) * x(i) \qquad (6)$$

Finite difference approximation method is applied to the partial differential equation system (PDEs) to solve the problem. Distance between nodes are considered as equal in nature and indices i and j were used to represent x and y directions. The distances between the points in the grid are considered as Δx, Δy in x and y directions respectively as shown in Figure 1 which portrays the computational grid with boundary conditions for the cylindrical model.
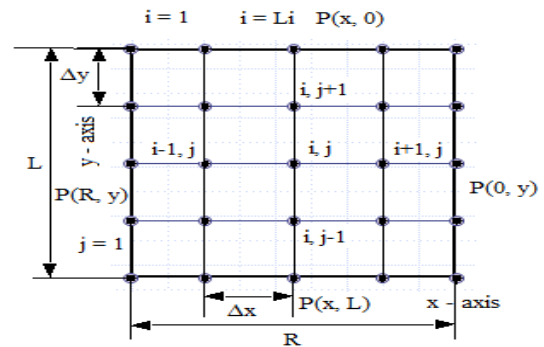

Figure 1. *Computational grid with boundary conditions for cylindrical model.*

Central difference scheme was used to approximate the second derivatives of pressure in space and backward difference method was used for first order of accuracy for space [26]. The resulting finite difference form of equation (1) assuming $\Delta x = \Delta y$ is given by

$$P_{i,j} = \frac{h^2\alpha(P_{i+1,j}) + P_{i,j+1} - P_{i,j-1} - \left[h^2\alpha\frac{h^2\alpha\Delta x}{x(i)}\right]P_{i-1,j}}{\left[2h^2\alpha - 2 - \frac{h^2\alpha\Delta x}{x(i)}\right]} \quad (7)$$

Elliptic PDEs are usually solved by approximation method which is most commonly approached by Gauss–Seidel iteration [26, 38]. The finite difference equation is applied at each node consecutively. Updated value from the previous node is used for each calculation. Relaxation method is used for repeated iterations until pressure distribution within a specified amount fails to change.

Over relaxation method is employed to accelerate the rate of convergence and obtain a stable equation by applying the following formula for each iteration.

$$P_{i,j}^{new} = w.P_{i,j}^{new} + (1-w)P_{i,j}^{old} \quad (8)$$

Here $P_{i,j}$ and $P_{i,j}^{old}$ are values of $P_{i,j}$ from the present and the previous iterations respectively , while w is the weighting factor in the range of 1 to 2 with an increment of 0.1 considered here. As with the conventional Gauss-Seidel method, the iterations are repeated until the absolute values of all the percent relative errors fall below a prespecified stopping criterion of 0.001. The percent relative errors are estimated by:

$$|(\varepsilon_s)| = \left|\frac{P_{i,j}^{new} - P_{i,j}^{old}}{P_{i,j}^{new}}\right| \text{X}100 \quad (9)$$

The finite difference (equation 7) form of the governing Laplace equation (1) employed with over relaxation method is solved using a 20 X 4 grid under axisymmetric conditions for the biomass in die under compressive load to analyse the pressure distribution inside the compact.

3.4. Compression Tests and Fracture Analysis

The internal strength of the manufactured pellets was analyzed by compression testing on both axial and diametrical directions. Compression tests were done on cured pellets by placing them on a disc shaped metal probe mounted on Instron universal testing machine (Model 3367; Instron Corporation, Canton, MA, USA) attached to a 20KN load cell. The test was run at 9 mm/min and stopped after pellet failure.

SEM was used to evaluate the bonding mechanism of the pellets. Compression test resulted in total breakage of the pellets. Fracture surfaces were prepared manually by breaking a pellet into two parts. Care was taken to replicate the way each pellet was fractured and that it took place in the same region. Care was taken to look at the surface a little distance from the end of the notch. Imaging was performed at the UNB Microscopy and Microanalysis Facility with a JEOL JSM-6400 Scanning Electron Micro-

scope. Samples were mounted onto an aluminum stub with double-sided carbon tape and carbon coated using (Edwards coating system E306A) carbon coater before observation in the microscope to prevent electric charging of the specimen.

4. Results and Discussion

4.1. MLR Modeling

The significance (p) values are shown (Table. 1) for RCG pellets of particle size 0.15 to 0.30 mm and particles less than 0.15mm.

Table 1. *Variance analysis of main factors and interaction terms.*

Source	RCG (P.S. 0.15 to 0.30mm)		RCG (P.S. 0 to 0.150mm)	
	DOF	p-value	DOF	p-value
Moisture content	1	0.001	1	0.049
Temperature	1	0.001	1	0.002
Pressure	1	0.049	1	0.040
Hold time	2	0.021	2	0.001
Moisture content * Temperature	1	0.001	1	0.003
Moisture content * Pressure	-	-	1	0.014
Temperature * Pressure	-	-	1	0.012
Error	17	-	15	-
SD	0.13		0.64	
R^2	99.4		95.7	

Test sample = 24 sets/species/P.S
Sources are reported only for p < 0.05.

MLR models obtained for RCG pellets with different particle sizes are as follows:

$F_{5, 18} = 593.58$, $p < 0.0005$ for RCG pellets with particle size 0.15 to 0.30 mm

$F_{7, 16} = 53.77$, $p < 0.0005$ for RCG pellets with particle size less than 0.15mm

For RCG pellets of particle size 0.15to 0.30mm,

$$L_{fp} = -31.1 - 0.00821H - 0.00456P$$
$$+ 4.53M + 0.586T - 0.0546MT.$$
$$(R^2 = 0.994)$$

For RCG pellets of particle size less than 0.15mm,

$$L_{fp} = 25.1 - 0.00646H - 0.0068P - 0.305M -$$
$$0.145T + 0.00725MT - 0.00155MP + 0.000327TP$$
$$(R^2 = 0.957)$$

The predicted values obtained using MLR modeling for length of pellet in die under compression were plotted against their respective experimental values as shown in figures 2 a & b which indicates excellent prediction capacity of the model with R2 values of 99% and 96% for RCG pellets of particle size 0.15 to 0.30mm and particles less than 0.15mm respectively. A sig (p) value of zero for the model shows that the independent variables were able to predict the dependent variable.

The effect of process parameters on length of pellet in die under compression can be analyzed using the main effects plot shown in fig. 3 for RCG pellets with their selected parameters. These plots show the effect of each independent variable on length of pellet in die under compressive load. It can be seen from fig. 3 that for RCG pellets with particle size 0.15 to 0.30mm an increase in moisture content lead to increase in length of pellet in die under compression. While an increase hold time and temperature helped increase the compression, not much difference was seen between the selected pressure ranges. Compression in RCG pellets made from particle size less than 0.15mm (Fig. 3.) was positively affected by an increase in hold time and temperature, whereas no big difference was seen in selected range of pressure and moisture.

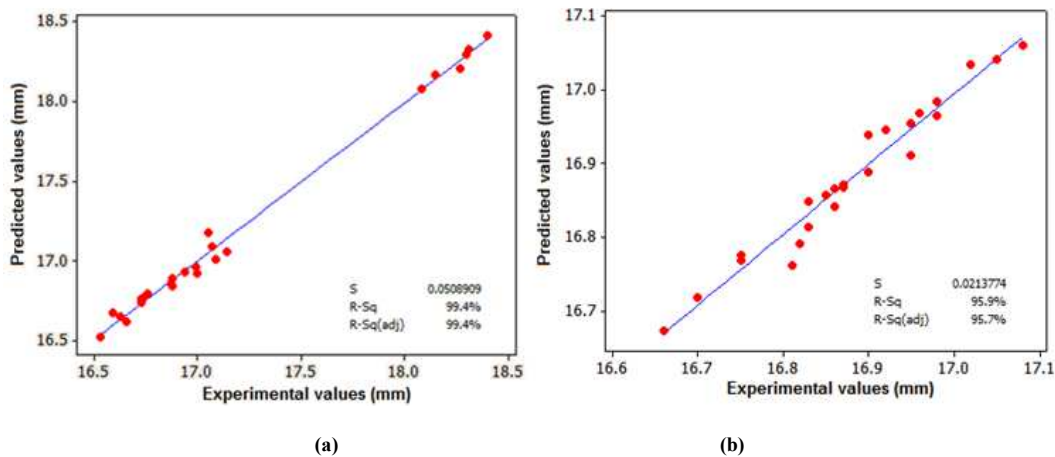(a)   (b)

Figure 2 a & b: Predicted values of regression model vs Experimental values of length of pellet in die under compression for pellets made from RCG with particle size 0.15 to 0.30mm and particles less than 0.15mm respectively.
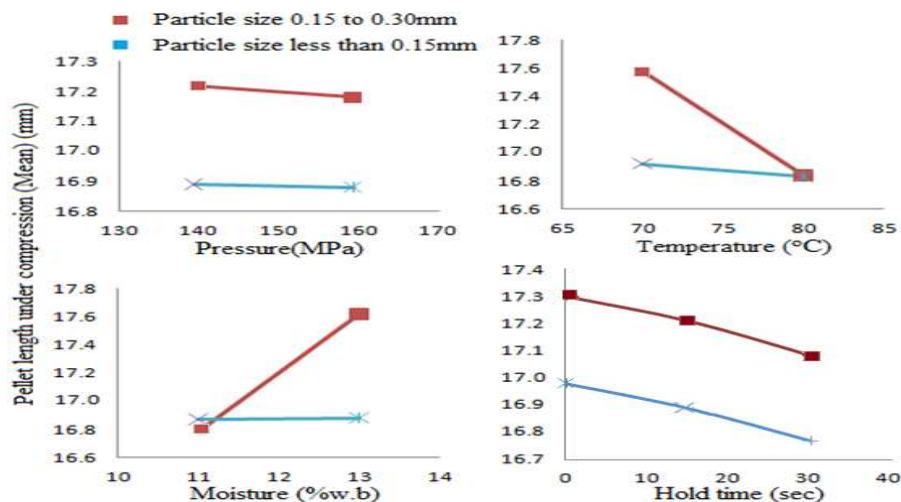

Figure 3. Main effects plot for length of pellet in die under compression (fitted means) for RCG with particle size 0.15 to 0.30mm and less than 0.15mm.

4.2. Springback Characteristics

Pellets made from RCG for different compression conditions involved in this study had a diameter of 8.08 to 8.12 mm (Appendix A) and there was not much difference in the diameter of the cured pellets comparatively. The length of the pellet under compressive loading ranged from 16.53 to 18.40mm, while the same for pellets immediately after extrusion were between 20.41mm to 22.70mm. The mean expansion in the length of pellets for selected parameters with particle size of 0.15 to 0.30mm was 25.72% (S.D = 2.67) while the same for 0 to 0.15mm were 25.29% (S.D = 1.06) for pellets made from RCG (Appendix A). This change in overall dimensions of pellets between the biomass under compression and extruded pellet is attributed towards the springback characteristics. While a large amount of expansion was noted between the feedstock under compressive load and extruded pellets, the same was

not true for the cured pellets which showed a mean expansion of 0.45% for pellets with particle size of 0.15 to 0.30mm while the same for 0 to 0.15mm was 0.3 % when compared to extruded pellets, which can be related to the operating temperatures as observed from a work based on corn stover and switch grass [12].

The unit pellet density of cured pellets ranged from 1074 – 1165 Kg m-3 for a compressive load of 139.3 and 159.2MPa. RCG pellets with particle size less than 0.15mm had the maximum density of 1164.89 Kg m-3 at moisture of 13% (w.b%), 80 oC, 159.2MPa and hold time of 15sec in the analyzed range of parameters (Fig. 4).

Expansion in length of green pellet when compared with pellets length under compressive load was lowest at (21.57%) at particle size 0.15 to 0.30mm at moisture 13% (w.b), 70 oC, 159.2MPa and hold time of 15sec.
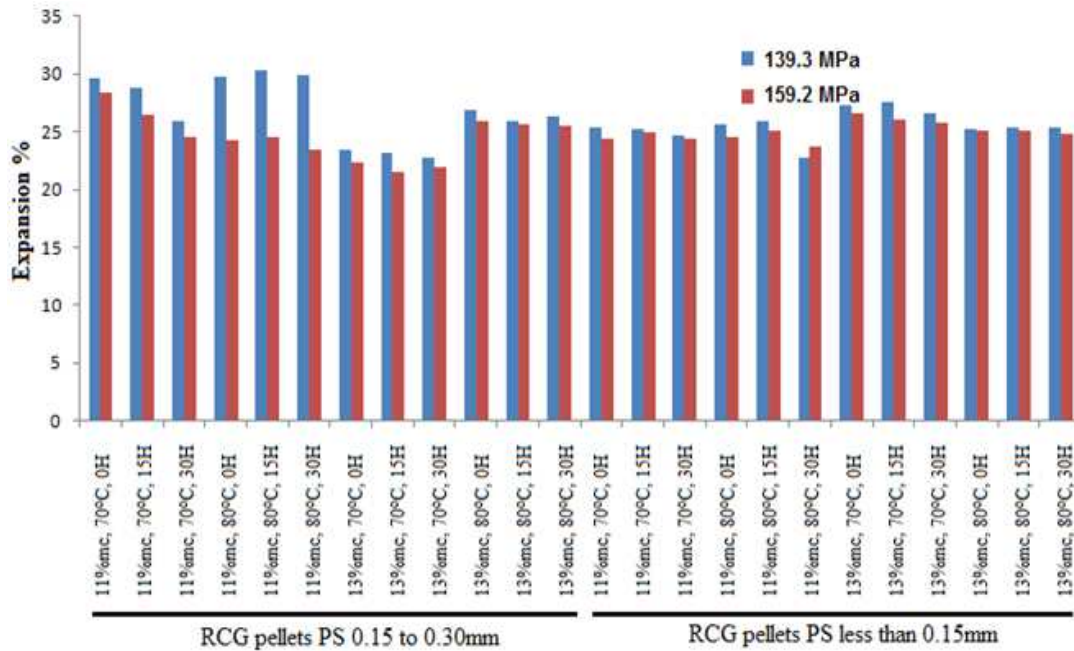

Figure 4: Expansion in RCG pellets with particle size 0.15 to 0.30mm and particles less than 0.15mm (mc – moisture content, H – hold time, PS – particle size).

4.2. Biomass Compaction Modeling by Finite Difference Method

Springback characteristics based on axial changes after the compaction process, which happens during decompacting and ejection stage from the die, was analysed, and a set of parameters that provide the least expansion were identified. Pellets with least expansion after the compressive load is released and the pellets were extruded from the die were considered for modeling. Expansion in compressed RCG was lowest (21.57%) at particle size 0.15 to 0.30mm at moisture 13% (w.b.), 70 oC, 159.2MPa and hold time of 15sec. Pressure distribution for pellets with parameters that lead to lowest expansion is shown in figure 5 for RCG biomass under compression. Aspect ratio for the RCG pellets was 0.44 respectively and coefficient of friction μ was 0.4 [32].

Figure 5 clearly explain that pressure distribution is not uniform throughout the compact although pressure at the top of the compact was uniform under the given loading conditions. It can also be understood that the pressure acting near the die wall is usually less than the corresponding centre.
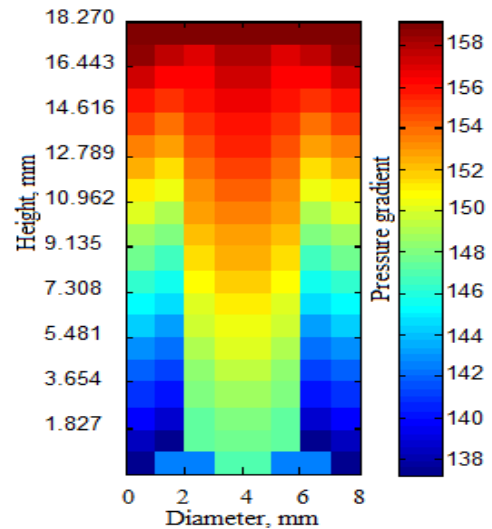

Figure 5. *Pressure distribution RCG biomass under compression for particle size 0.15 to 0.30mm at moisture 13% (w.b.), 70°C, 159.2MPa and hold time of 15sec.*

whose cause can be attributed towards friction between the die wall and particles. It can be noted that under compressive load, a low pressure zone is created around the die wall in the compact at the bottom which is approximately

86% for RCG.

A differential pressure distribution during compaction process is caused by the friction which exists between the powder and the die wall and the radial forces acting on the die wall due to uniaxial compressive loading. This phenomenon causes a density gradient in the compacted biomass which can be analysed by the following equation [26, 29]

$$\rho = \rho_o + k.P^{1/3} \qquad (10)$$

Where ρ_o is initial relative density and k is a constant reflecting variations in material properties such as hardness and plasticity. Soft and ductile powders have higher *k* values than hard and brittle powders. Bejarano. et.al, [39] derived a correlation between yield strength (σ_y) and *k* based on the latter's descriptive property for deformation which was also highlighted by Mohammed et al. [26].

$$\sigma_y = \frac{1}{3}k \qquad (11)$$

The reciprocal of the slope k has been found to reflect the yield pressure P_y of a material. This means that the yield pressure P_y of a material is equal to $3\sigma_y$ [29, 40].

Figure.6 demonstrates the density distribution through contour maps. During the compression process there is a large increase in initial density under low pressure which is due to the initial arrangement of the particles, after which actual densification takes place.   It shows that there are well defined regions of high density at the top of the compact. It can also be seen that the density distribution is not uniform throughout the compact. It has been realised that a density difference of about 4% exists throughout the compact. While the distribution is even at the top of the compact, it is not the same at the bottom because of the pressure difference due radial and frictional forces caused by uniaxial loading condition.
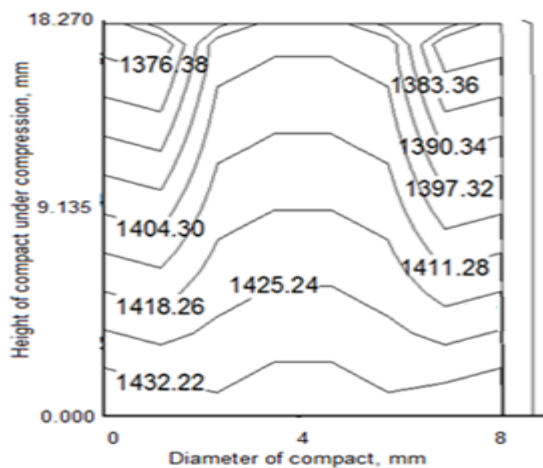

Figure 6. Density contour maps for RCG biomass under compression (density in kg m^{-3}) for particle size 0.15 to 0.30mm at moisture 13% (w.b.), 70°C, 159.2MPa and hold time of 15sec.

(*Note: Density contour shows the bottom part as top of the compact and vice versa)

4.2. Compressive Strength and Fracture Analysis

Compression tests for pellets made with selected parameters were conducted and parameters providing results for highest strength are reported. RCG pellets with particle size 0.150mm to 0.300mm with 10% moisture at 80°C under a compressive load of 159.2MPa had took an axial compressive load of 2.43 ± 0.10KN before breaking which was the highest for pellets made with selected parameters. RCG pellets were able to withstand a diametrical compressive load of 0.91 ±0.04KN which came in the form of pellets made from particle size less than 0.150mm with moisture of 13% at 80°C under a compressive load of 159.2MPa during compaction

SEM image of RCG pellet made from with particle size 0.150mm to 0.300mm with 10% moisture at 80°C under a compressive load of 159.2MPa (Fig 7) showed a lot of inter particle gaps and voids which leads to poor adhesion between particles. This can be related to lower strength of RCG pellets when compared to wood pellets. Uneven fracture surface as seen in figure 7 may have been due to the energy intense fracture mechanism which is indicative of cohesive failure of the solid lignin bridge [30].
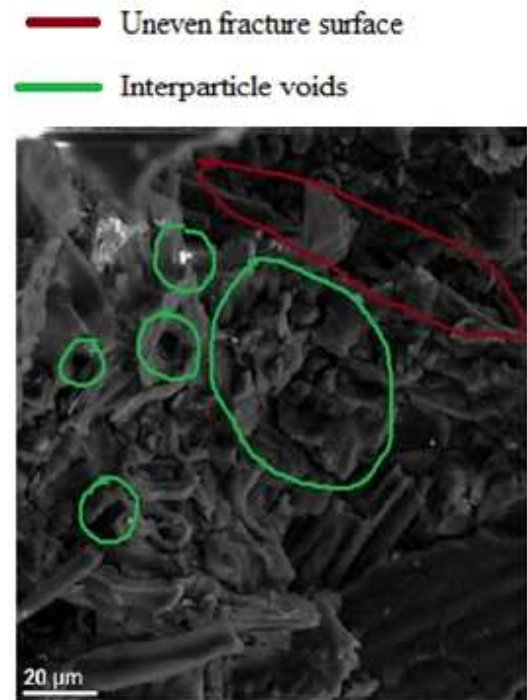
Figure 7. High magnification SEM image of fractured RCG pellet.

5. Conclusions

The effect of selected individual parameters on the length of pellet under compressive load was analysed and their compression characteristics in a closed end die in the analyzed range are presented.

MLR model developed with the help of selected feedstock and process parameters consisting of hold time, pressure, moisture content, and temperature as main factors along

with their interaction terms predicted the length of pellet under compressive load with an accuracy of 99% and 96% for RCG pellets with particle size 0.15 to 0.30mm and particles less than 0.15mm respectively.

Springback characteristics based on axial changes after the compaction process which happens during decompacting and ejection stage from the die was analysed and parameters which provide the least expansion and higher density are identified. RCG pellets with particle size less than 0.15mm had the maximum density of 1164.89 Kg m^{-3} at moisture of 13% (w.b%), 80 ºC, 159.2MPa and hold time of 15sec. Expansion was lowest for RCG pellets lowest (21.57%) at particle size 0.15 to 0.30mm at moisture 13% (w.b), 70 ºC, 159.2MPa and hold time of 15sec.

Pressure and density distributions of biomass under compressive load was analysed by finite difference method. The compact geometry and friction between particles and die wall had effects on the pressure and density distributions in the compacted biomass. Pressure and density at the top of the compact are higher compared to the bottom at the die wall. The analysis also shows that in the radial direction there is an increase in density leading to the central axis in the upper region of the compact

SEM analysis of RCG pellets showed inter particle gaps and voids which lead to poor adhesion between particles and uneven fracture surface due to the energy intense fracture mechanism.

Acknowledgements

Appendix: A Compaction characteristics of RCG pellets

Hold Time, (s)	Pressure, (MPa)	Moisture Content, (%wb)	Temperature, (ºC)	pellet length in die under compression, (mm) Mean	SD	extruded pellet length (mm)	pellet diameter after extrusion, (mm)	expansion after(length) extruded pellet, %	density of inextruded pellet, Kg/m³	cured pellet length, (mm)	expansion in cured pellet, %	density of cured pellet, (Kg/m³)
Pellets made from RCG of 0.15 to 0.3mm particle size												
0.00	139.26	11.00	70.00	17.09	0.05	22.16	8.10	29.67	1113.26	22.22	0.27	1086.50
15.00	139.26	11.00	70.00	16.88	0.08	21.74	8.11	28.79	1133.84	21.85	0.50	1099.34
30.00	139.26	11.00	70.00	16.73	0.04	21.07	8.11	25.94	1158.04	21.20	0.61	1122.91
0.00	159.16	11.00	70.00	17.00	0.06	21.82	8.10	28.35	1130.78	21.93	0.50	1091.40
15.00	159.16	11.00	70.00	16.76	0.08	21.20	8.10	26.49	1149.85	21.25	0.24	1133.08
30.00	159.16	11.00	70.00	16.59	0.04	20.65	8.09	24.47	1184.53	20.82	0.82	1147.85
(Note: intermediate data was intentionally cut to save space)												
0.00	139.26	13.00	80.00	17.05	0.07	21.64	8.10	26.92	1150.32	21.79	0.69	1117.20
15.00	139.26	13.00	80.00	17.14	0.03	21.58	8.09	25.90	1157.73	21.64	0.28	1126.02
30.00	139.26	13.00	80.00	16.94	0.05	21.41	8.10	26.39	1164.49	21.51	0.46	1133.64
0.00	159.16	13.00	80.00	17.07	0.08	21.49	8.10	25.89	1159.34	21.57	0.37	1127.79
15.00	159.16	13.00	80.00	16.99	0.06	21.35	8.10	25.66	1171.13	21.41	0.28	1140.11
30.00	159.16	13.00	80.00	16.88	0.04	21.18	8.10	25.47	1172.74	21.29	0.52	1142.44
Pellets made from RCG of 0 to 0.15mm particle size												
0.00	139.26	11.00	70.00	17.08	0.05	21.40	8.08	25.29	1175.28	21.43	0.14	1135.14
15.00	139.26	11.00	70.00	16.98	0.08	21.27	8.09	25.27	1178.26	21.32	0.23	1135.71
30.00	139.26	11.00	70.00	16.87	0.06	21.03	8.10	24.66	1163.48	21.09	0.28	1146.00
0.00	159.16	11.00	70.00	17.05	0.08	21.20	8.08	24.34	1166.77	21.23	0.14	1142.16
15.00	159.16	11.00	70.00	16.92	0.05	21.15	8.08	25.00	1184.10	21.19	0.19	1143.49
30.00	159.16	11.00	70.00	16.83	0.07	20.94	8.08	24.42	1199.70	21.01	0.33	1155.05
(Note: intermediate data was intentionally cut to save space)												
0.00	139.26	13.00	80.00	16.98	0.06	21.27	8.09	25.27	1169.57	21.35	0.37	1131.39
15.00	139.26	13.00	80.00	16.90	0.08	21.19	8.10	25.38	1172.19	21.27	0.38	1120.98
30.00	139.26	13.00	80.00	16.82	0.05	21.08	8.11	25.33	1180.36	21.15	0.33	1133.53
0.00	159.16	13.00	80.00	16.96	0.07	21.21	8.09	25.06	1175.17	21.33	0.56	1129.80
15.00	159.16	13.00	80.00	16.87	0.03	21.09	8.09	25.01	1173.37	21.14	0.24	1164.89
30.00	159.16	13.00	80.00	16.75	0.05	20.90	8.10	24.78	1188.54	20.97	0.33	1146.45

References

[1] McKendry, P. (2002). Energy production from biomass (part 1): overview of biomass. Bioresource Technology 83(1), 37-46.

[2] Larsson, S. H., Thyrel, M., Geladi, P., and Lestander, T. A. (2008). "High quality biofuel pellet production from pre-compacted low density raw materials," Bioresource Technology 99(15), 7176-7182.

[3] Lewandowski I; Kicherer A. (1997). Combustion quality of biomass: practical relevance and experiments to modify the biomass quality of Miscanthus × giganteus. European Journal of Agronomy;6:163–77.

[4] Marten GC; Jordan RM & Hovin AW. Biological significance of reed canary grass (Phalaris arundinacea) alkaloids and associated palatability variation to grazing sheep and cattle. Agronomy Journal 1976;68:909–14.

[5] Østrem L., (1987). Studies on genetic variation in reed canary grass, Phalaris arundinacea L. I. Alkaloid type and concentration. Hereditas;107:235–48.

[6] Hadders G, Olsson R. (1997). Harvest of grass for combustion in late summer and spring. Biomass and Bioenergy 12(3): 171–5.

[7] Lewandowski, I; Scurlock, J.M.O; Lindvall, E. & Christou, M.U. (2003). The development and current status of perennial rhizomatous grasses as energy crops in the US and Europe. Biomass and Bioenergy 25(4), 335-361.

[8] Burvall J; Hedman B (1994). Fuel characteristics of Reed canary grass—results from third and second years, Swedish Institute of Agricultural Engineering.

[9] Rumpf H (1962). The strength of granules and agglomerates. In: Agglomeration (Knepper W A ed), pp. 379–419. John Wiley and Sons, New York, NY.

[10] Amarnath Dhamodaran., Muhammad T.Afzal (2012). Compression and springback properties of hardwood and softwood pellets. Bioresources 7(3) 4362-4376.

[11] Kaliyan N; Morey R V (2006). Densification Characteristics of Corn Stover and Switchgrass. ASABE Paper No.066174. American Society of Agricultural and Biological Engineers (ASABE), St. Joseph, MI.

[12] Kaliyan N; Morey R V (2009). Constitutive model for densification of corn stover and switchgrass. Bio systems engineering (2009), 47 – 63.

[13] Kremmer, M. and J. F. Favier. (2001). A method for representing boundaries in discrete element modeling-Part II: Kinematics. International Journal for Numerical Methods in Engineering 51: 1423-1436.

[14] Cundall, P. A and O. D. L. Strack. (1979). A discrete numerical model for granular assemblies. Geotechnique 29 (1): 47 – 65.

[15] Tripodi M A; Puri V M; Manbeck H B; Messing G L (1992). Constitutive models for cohesive particulate materials. Journal of Agricultural Engineering Research, 53(1), 1–21.

[16] Peleg M; Bagley E B (1983). Physical Properties of Foods. AVI Publishing Company, Inc., Westport, CT.

[17] Drucker D C; Prager W (1952). Soil mechanics and plastic analysis or limit design. Quarterly of Applied Mathematics, 10(2), 157–165.

[18] Schofield A N; Wroth C P (1968). Critical State Solid Mechanics. McGraw Hill, New York, NY.

[19] DiMaggio F L; Sandler I S (1971). Material model for granular soils. Journal of Engineering Mechanics ASCE, 96, 935–950.

[20] Procopio, A.T., Zavaliangos, A., Cunningham, J.C. (2003). Analysis of the diametrical compression test and the applicability to plastically deforming materials. Journal of Materials Science 38, 3629–3639.

[21] Aydin, I., Briscoe, B.J., Sanliturk, K.Y., (1996). The internal form of compacted ceramic components: a comparison of a finite element modeling with experiment. Powder Technology 89, 239–254.

[22] Michrafy, A; Ringenbacher, D; Tchoreloff, P. (2002). Modeling the compaction behaviour of powders: application to pharmaceutical powders. Powder Technology 127 (3), 257–266.

[23] Sinka, I.C., Cunningham, J.C., Zavaliangos, A. (2003). The effect of wall friction in the compaction of pharmaceutical tablets with curved faces: a validation study of the Drucker-Prager cap model. Powder Technology 133 (1–3), 33–43.

[24] Cunningham, J.C., Sinka, I.C., Zavaliangos, A., (2004). Analysis of tablet compaction. I. Characterization of mechanical behavior of powder and powder/tooling friction. Journal of Pharmaceutical Sciences 93 (8), 2022–2039.

[25] Wu, C.Y., Ruddy, O.M., Bentham, A.C., Hancock, B.C., Best, S.M., Elliott, J.A. (2005). Modeling the mechanical behaviour of pharmaceutical powders during compaction. Powder Technology 152 (1–3), 107–117.

[26] Mohammed Jasim Kadhim k; Adil A. Alwan; Iman J. Abed. (2011). Simulation of cold die compaction alumina powder. Trends in Mechanical Engineering& Technology Volume Pages 1-21. 1:1, 1-21.

[27] Secondi J. (2002). Modeling powder compaction: From a pressure-density law to continuum mechanics. Powder Metallurgy. 45. 213-217p.

[28] Gaboriault E. M. (2003). The effects of fill-nonuniformities on the densified states of cylindrical green P/M compacts MSc Thesis. Department of Mechanical Engineering, Worchester Polytechnic Institute, USA.

[29] Mahoney F. M. and Readey M. J. (1995). Applied mechanics modeling of granulated ceramic powder compaction. Conference: 27 International Society for the Advancement of Materials and Process Engineering (SAMPE) Technical conference, Albuquerque, NM, USA. 10-12.

[30] Stelte W, Jens K. Holm, Anand R. Sanadi, Soren Barsberg, Jesper Ahrenfeldt, Ulrik B. Henriksen (2010). A study of bonding and failure mechanisms in fuel pellets from different biomass resources. biomass and bio energy 35 910 – 918.

[31] Kaliyan N; Morey R V (2009). Natural binders and solid bridge type binding mechanisms in briquettes and pellets made from corn stover and switchgrass. Bioresource Technology 101. 1082–1090.

[32] Larsson, S. H (2009). "Kinematic wall friction properties of reed canary grass powder at high and low normal stresses," Powder Technology 198 108–113.

[33] Ready M. J. (1995) "Compaction of spray-dried ceramic powders: an experimental study of the factors that control green density" International (SAMPE) Technical conference series. Edited R. J. Martinez, H. 27.

[34] Crawford R. J. and Sprevak D. (1984) European Polymer Journal. 5. 441-446p.

[35] Pease L. F. (2005). A quik tour of powder metallurgy. Advanced Materials and Processes. 163:36-38.

[36] Collins II G. W. (2003). "Fundamental numerical methods and data analysis" NASA Astrophysics Data System (ADS) USA. 25-50p.

[37] Brewin P, R; Coube, O; Doremus, P and Tweed, J.H. (2008). Modeling of powder die compaction, Springer.

[38] Shima S. and Saleh M. (1993) Variation of density distribu-

tion in compacts in lose die compaction with powder cha-racteristics, Advanced in powder metallurgy and Particulate materials, modeling design and computational methods Nashville, Tennessee, USA. 175-188.

[39] Bejarano A; Riera M.D and Prado JM (2003). Simulation of compaction process of a two level powder metallurgical part. Journal of Materials Processing Technology 2003. 143-144:34-40.

[40] Scott, J. E.; Kenkre, V. M. and Hurd, A. J. (1998) Nonlocal approach to the analysis of the stress distribution in granular systems. II. Application to experiment. Physical Review E 57 (5) 5850-5857.